Natural-convection heat transfer in an inclined porous layer boarded by a finite-thickness wall

M. Mbaye, E. Bilgen and P. Vasseur
Department of Mechanical Engineering, Ecole Polytechnique de Montréal, Montreal, Canada

In this paper, natural-convection heat transfer in an inclined porous layer boarded by a wall with finite thickness and conductivity is studied both analytically and numerically. A constant heat flux is applied for heating and cooling the long side walls of the rectangular enclosure while the other two walls are insulated. Several different flow models for porous media are considered, such as Brinkman-extended Darcy and Forschheimer–Brinkman-extended Darcy models. The governing equations, derived from the Brinkman-extended Darcy formulation, are solved analytically, in the limit of a thin system, using the parallel flow approximation. Results are obtained in terms of an overall Nusselt number as a function of Rayleigh and Darcy numbers, angle of inclination of the system, and thickness and conductivity of the bordering wall. The analytical solution is compared with the numerical results obtained by solving the complete system of governing equations. An analysis is made on the proper choice of parameters that can describe the criteria for the range of validity of Brinkman-extended Darcy's law in this type of configuration.

Keywords: inclined cavity; natural-convection; porous media

Introduction

Natural convection in porous media has been studied extensively over the past 20 years or so due to several important geophysical and engineering applications. These include energy conservation in buildings, water movements in geothermal reservoirs, and solar collector applications. An excellent review of existing experimental and numerical results has been presented by Combarnous and Bories (1975) and Cheng (1978), among others.

Most analytical studies for natural convection in porous media are based on Darcy's law. The most common reason for the wide use of a Darcian formulation is its simplicity. However, the few available experimental studies of heat transfer in vertical porous cavities (see, for instance, Klarsfeld 1970; Bories and Combarnous 1973; Seki et al. 1978) have never agreed with the theoretical results obtained with the Darcy model. Extensive efforts have thus been made to include the viscous diffusion and inertia terms in the governing equations in recent studies of natural convection in porous media.

To account for the boundary effect, which may become important in some situations, Brinkman's extension of Darcy's law must be used. The Brinkman equation removes some of the deficiencies of Darcy's law, since it can satisfy all the boundary conditions at a solid surface or a fluid interface. Chan et al. (1970) used the Brinkman model to study natural convection in a rectangular porous box that is differentially heated in the horizontal direction. Their numerical computations indicate that when the Darcy number based on the width of the enclosure is less than 10^{-3}, the results are in good agreement with Darcy's law. A boundary-layer analysis for natural convection in a vertical porous layer was performed by Tong and Subramanian (1985). The boundary-layer equations, derived from the Brinkman model, were solved using the modified Oseen method (see, for instance, Weber 1975). It was found that the pure Darcy analysis is applicable only when $R\,\mathrm{Da}/A < 10^{-4}$. The same problem was considered numerically by Lauriat and Prasad (1987). It was shown that for a fixed modified Rayleigh number, the Nusselt number decreases with an increase in the Darcy number, the reduction being larger at higher values of the Rayleigh number. Similar results have been obtained both theoretically and numerically by Vasseur et al. (1987a) for a vertical cavity heated and cooled with uniform heat fluxes along its vertical side walls. Natural convection in a shallow porous cavity has been studied analytically by Sen (1987) and Vasseur et al. (1989a), respectively, for various thermal and hydrodynamic boundary conditions. For Darcy numbers higher than 10^{-4}, the resulting Nusselt numbers were found to be significantly smaller than the values predicted by Darcy's law.

It is now well known that the Darcy flow model breaks down when the inertia resistance becomes comparable to the Darcy viscous resistance. Forschheimer (1901) proposed a quadratic term in Darcian velocity to describe the inertia effects. Poulikakos and Bejan (1985a, 1985b) investigated the inertia effects through the inclusion of the Forschheimer's extension. Beckerman et al. (1986) have shown that at high Darcy numbers the inertia and viscous terms must be included simultaneously to obtain realistic predictions of the heat transfer. Recently, Lauriat and Prasad (1987) used Brinkman's and Forschheimer's extensions of Darcy's law to study non-Darcian natural convection in a differentially heated vertical cavity. It was found that a porous medium can transport more energy than a saturating fluid alone if the porous matrix is highly permeable and the thermal conductivity of solid particles is greater than that for the fluid.

The purpose of the present work is to study the natural-convection heat transfer in an inclined porous layer

Address reprint requests to Professor Vasseur at the Department of Mechanical Engineering, Ecole Polytechnique de Montréal, C.P. 6079, Succ. "A" Montreal, P.Q., H3C 3A7, Canada.

Received 8 June 1992; accepted 14 January 1993

boarded by a solid wall of finite thickness and conductivity, and heated from the sides by a constant heat flux. This type of configuration is of interest in several engineering applications. These include building-insulation layers, the design of solar collectors, the solidification process in porous media, etc. Most of the studies available in the literature on natural convection in porous-media enclosures are concerned with the numerical study of a vertical layer heated isothermally from the sides. However, in many applications the isothermal-walls model is clearly inadequate. For instance, the temperature of the great majority of walls encountered in architectural and solar applications is not maintained uniform; rather, it is the consequence of the heat flux imposed to the wall. Also, the present investigation takes into account the effect of inclination of the system and the influence of a boarding wall. These two parameters are important in many practical situations.

Our analysis proceeds as follows. First, we derive a closed-form analytical solution valid in the limit of a shallow system ($A \gg 1$). The porous medium is modeled using the Brinkman-extended Darcy equations. Our mathematical treatment parallels that of Vasseur et al. (1987b, 1989a) who have considered the case of an inclined porous layer in the absence of a boarding wall. This is followed by a numerical solution of the full governing equations, which include both the Forschheimer and Brinkman modifications. The relative importance of inertia and viscous forces is discussed. The numerical results are used to establish criteria for deviation from the Darcy and Brinkman-extended Darcy solutions.

Formulation of the problem

The physical situation and coordinate system is depicted in Figure 1. The enclosure of height H' and thickness L' is boarded

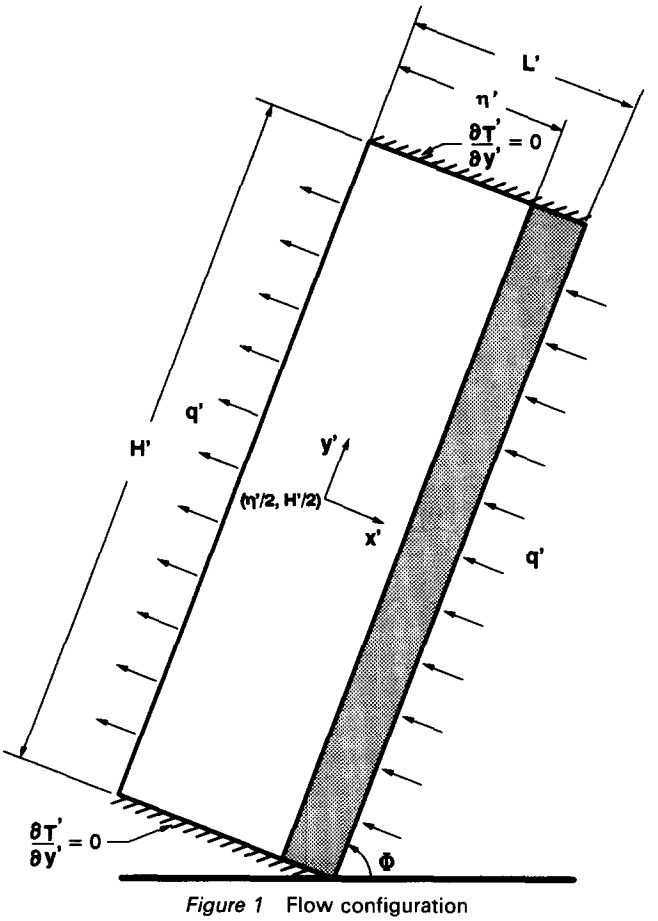

Figure 1 Flow configuration

Notation

A	Aspect ratio $= H'/L'$
b'	Matrix structure property associated with the Forschheimer term, m
C	Dimensionless temperature gradient along y-direction
c	Specific heat at constant pressure, $J \cdot kg^{-1} \cdot K^{-1}$
Da	Darcy number $= K'/L'^2$
Fs	Forschheimer number $= b'/L'$
g	Acceleration due to gravity, $m \cdot s^{-2}$
H'	Cavity height, m
K'	Permeability of porous matrix, m^2
k_f	Thermal conductivity of fluid, $W \cdot m^{-1} \cdot K^{-1}$
k_p	Thermal conductivity of porous medium, $W \cdot m^{-1} \cdot K^{-1}$
k_s	Thermal conductivity of solid wall, $W \cdot m^{-1} \cdot K^{-1}$
L'	Cavity width, m
Nu	Nusselt number $= \Delta T_c/\Delta T$
p	Dimensionless pressure $= p'K/\mu\alpha_p$
Pr	Fluid Prandtl number $= \nu/\alpha_f$
Pr*	Porous Prandtl number $= \nu/\alpha_p$
q'	Constant heat flux, $= W \cdot m^{-2}$
Ra	Fluid Rayleigh number $= g\beta q' L'^4/\nu\alpha_f k_f$
R	Darcy–Rayleigh number $= g\beta K' L'^2 q'/\nu\alpha_p k_p$
T'_0	Reference temperature at $x' = y' = 0$, K
T	Dimensionless temperature $= (T' - T'_0)/\Delta T'$
u, v	Dimensionless fluid velocity components $= u'L/\alpha_p$, $v'L/\alpha_p$
x, y	Dimensionless Cartesian coordinates $= x'/L'$, y'/L'

Greek symbols

α_f	Thermal diffusivity of fluid $= k_f/(\rho c)_f$, $m^2 \cdot s^{-1}$
α_p	Thermal diffusivity of porous medium $= k_p/(\rho c)_f$, $m^2 \cdot s^{-1}$
β	Isobaric coefficient of thermal expansion of fluid, K^{-1}
$\Delta T'$	Temperature difference $= q'L'/k_p$, K
ΔT	Wall-to-wall dimensionless temperature difference $T(-\eta/2, 0) - T(1 - \eta/2, 0)$
ε	Porosity
η	Dimensionless thickness of porous layer $= \eta'/L'$
θ	Dimensionless temperature
κ	Relative conductivity $= k_s/k_p$
λ	Relative viscosity $= \mu_{eff}/\mu$
μ	Dynamic viscosity of fluid, $kg \cdot m^{-1} \cdot s^{-1}$
μ_{eff}	Apparent dynamic viscosity for Brinkman's model, $kg \cdot m^{-1} \cdot s^{-1}$
ν	Kinematic viscosity of fluid, $m^2 \cdot s^{-1}$
ρ	Fluid density, $kg \cdot m^{-3}$
Φ	Angle of inclination of the enclosure
ψ	Dimensionless stream function $= \psi'/\alpha_p$

Subscripts

f	Fluid
p	Fluid saturated porous medium
s	Solid
c	Pure conduction

Superscript

'	Dimensional variables

by a solid wall of extension $(L' - \eta')$, and the system is tilted at an angle Φ with respect to the horizontal. The two end walls are insulated, while a uniform heat flux q' is applied along both side walls. The thermophysical properties of the fluid are assumed constant, except for the density in the buoyancy term in the momentum equations. The porous medium is considered homogeneous and isotropic and is saturated with a fluid that is in local thermodynamic equilibrium with the solid matrix.

Assuming that the flow is steady and two-dimensional (2-D), the governing equations, in terms of the superficial (Darcian) velocity, can be written as follows (Beckerman et al. 1986):

$$\frac{\partial u'}{\partial x'} + \frac{\partial v'}{\partial y'} = 0 \tag{1}$$

$$\frac{\partial p'}{\partial x'} = \mu_{\text{eff}} \nabla^2 u' - \frac{u'}{K'}(\mu + \rho b' |\vec{V}'|) - \rho g \beta (T' - T'_0) \cos \Phi \tag{2}$$

$$\frac{\partial p'}{\partial y'} = \mu_{\text{eff}} \nabla^2 v' - \frac{v'}{K'}(\mu + \rho b' |\vec{V}'|) - \rho g \beta (T' - T'_0) \sin \Phi \tag{3}$$

$$(\rho c)_f \left[u' \frac{\partial T'}{\partial x'} + v' \frac{\partial T'}{\partial y'} \right] = k_p \nabla^2 T' \tag{4}$$

where $|\vec{V}| = \sqrt{u'^2 + v'^2}$ and b' is the inertial coefficient. All the other symbols in the above equations are defined in the nomenclature.

Equations 1–4 may be rendered dimensionless by employing the following scales: L' for length, $\mu\alpha_p/K'$ for pressure, α_p/L' for velocity and $q'L'/k_p$ for temperature. We obtain

$$\frac{\partial u}{\partial x} + \frac{\partial v}{\partial y} = 0 \tag{5}$$

$$\frac{\partial p}{\partial x} = \lambda \, \text{Da} \, \nabla^2 u - u(1 + \Lambda |\vec{V}|) - RT \cos \Phi \tag{6}$$

$$\frac{\partial p}{\partial y} = \lambda \, \text{Da} \, \nabla^2 v - v(1 + \Lambda |\vec{V}|) + RT \sin \Phi \tag{7}$$

$$u \frac{\partial T}{\partial x} + v \frac{\partial T}{\partial y} = \nabla^2 T \tag{8}$$

where $|\vec{V}| = \sqrt{u^2 + v^2}$ and $\Lambda = \text{Fs}/\text{Pr}^*$.

The boundary conditions are given in dimensionless form as

$$u = v = 0 \qquad \text{on all solid boundaries} \tag{9a}$$

$$y = \pm A/2 \qquad \frac{\partial T}{\partial y} = 0, \tag{9b}$$

$$x = -\eta/2, 1 - \eta/2 \qquad \frac{\partial T}{\partial x} = 1, \kappa^{-1} \tag{9c}$$

$$x = \eta/2 \qquad T^+ = T^-; \left.\frac{\partial T}{\partial x}\right|^- = \kappa \left.\frac{\partial T}{\partial x}\right|^+ \tag{9d}$$

Equations 9b and 9c result from the thermal boundary conditions applied on the enclosure, while Equation 9d express the continuity of temperature and heat flux at the interface between the solid wall and the porous matrix.

From the dimensionless equations (Equations 5–9), it is seen that the present problem is governed by height parameters, namely R, Da, Λ, λ, κ, η, A, and Φ. However, in the present study, the value of μ_{eff} in Brinkman's extension is taken, as a first approximation, equal to μ (i.e., $\lambda = 1$).

The heat transfer across the system can be expressed in term of a Nusselt number at $y = 0$, defined as

$$\text{Nu} = \frac{\Delta T_c}{\Delta T} \tag{10}$$

where ΔT is the dimensionless temperature difference across the section, and ΔT_c is the corresponding temperature difference for pure conduction $(\Delta T_c = 1 + (1 - \eta)(\kappa^{-1} - 1))$.

Numerical solution

The numerical solution of governing equations 5–8 is obtained using the SIMPLER algorithm (Patankar 1980). The control-volume formulation used in the algorithm ensures continuity of the convective and diffusive fluxes as well as overall momentum and energy conservation. The mesh size required for sufficient numerical accuracy depends mainly on the Rayleigh and Darcy numbers. A mesh of 25 × 25 to 75 × 75 nodal points ensured independence of solution on the grid. The nodal points were uniformly distributed in the y-direction, while the distribution along the x-direction was slightly skewed to obtain a greater concentration of points near the heated and cooled boundaries. The convergence criteria were based on the corrected pressure field. When the corrected terms were small enough so that no difference existed between the pressure field before and after correction ($\Sigma b_{ij} < 10^{-4}$), the computation was stopped. For small Rayleigh numbers, the number of iterations was about 50. For larger R, the solution from the smaller R was used to initialize the computation so the number of iterations was reduced considerably. Besides the usual control, the accuracy of computations was controlled using the energy conservation within the system.

A test of the accuracy of the present numerical algorithm was obtained by comparing the results to those reported in the literature for the limiting case of a fully porous vertical enclosure with the vertical walls held at different temperatures and the connecting horizontal walls maintained adiabatic. Tables 1a and 1b show that the present numerical model is in good agreement with the Darcy–Brinkman and the Darcy–Brinkman–Forschheimer solutions reported in the literature by various authors. For instance, Table 1b indicates that for $R = 10^4$, $\text{Da} = 10^{-4}$ and $\text{Pr} = 1$, the present solution for the Darcy–Brinkman–Forschheimer model ($b'/\sqrt{K'} = 0.55$) agrees to within 0.5 percent and 3 percent with the results reported by Lauriat and Prasad (1989) and Beckerman et al. (1986), respectively. For this situation the strength of convection is extremely high ($\text{Nu} \simeq 18$) and a mesh of 112 × 112 was necessary to ensure independence of the solution with respect to the number of grid points. Also, some of the cases considered by Vasseur et al. (1987a) for the case of a vertical Brinkman layer heated from the sides by constant heat fluxes were reproduced. In general it was found that essentially identical

Table 1a Nusselt number with Brinkman-extended Darcy flow model ($A = 1.0$)

R	Da	Pr	Present	Ettefagh et al. (1991)	Lauriat et al. (1989)	Beckerman et al. (1986)
10^4	10^{-1}	1.0	4.69	—	4.68	4.72
10^4	10^{-1}	10^{-2}	4.69	—	4.68	4.72
10^4	10^{-4}	1.0	25.42	—	25.70	24.97
10^4	10^{-4}	10^{-2}	25.42	—	25.70	24.97
10^3	10^{-5}	1.0	12.42	12.64	—	—

Table 1b Nusselt number with Forschheimer–Brinkman-extended Darcy flow model ($A = 1.0$)

R	Da	Fs/Pr*	Present	Ettefagh et al. (1991)	Lauriat et al. (1989)	Beckerman et al. (1986)
10^4	10^{-1}	1.74×10^{-1}	4.39	—	4.36	4.39
10^4	10^{-1}	1.74×10^{1}	1.94	—	1.94	1.94
10^4	10^{-4}	5.5×10^{-3}	18.49	—	18.40	20.59
10^4	10^{-4}	5.5×10^{-1}	6.11	—	6.19	6.02
500	0	0	9.02	8.98	—	—
500	0	10^{-4}	8.93	8.92	—	—
500	0	5×10^{-4}	8.65	8.67	—	—
500	0	10^{-3}	8.46	8.44	—	—

flow and temperature patterns as well as the average heat transfer were obtained. For instance, when $R = 500$ and $\mathrm{Da} = 10^{-4}$, an overall Nusselt number of 5.386 was obtained in the present study, while that reported by Vasseur et al. (1987a) was 5.398.

With thermal boundary conditions of uniform heating, the convective motion becomes independent of aspect ratio A for large aspect ratios (Vasseur et al. 1987b). Other numerical tests using various aspect ratios A were done while other conditions, including the mesh size, were maintained constant. It was found that Nu converges very fast to an asymptotic value when $A \geq 4$. For this reason, all the numerical results presented here were obtained for $A = 4$.

Approximate analytical solution

In this section an approximate solution, valid for the Brinkman-extended Darcy regime ($\mathrm{Fs} = 0$), is presented for the case of a long shallow system ($A \gg 1$). In this limit, as discussed in detail by Cormack et al. (1974), Walker and Homsy (1978), Vasseur et al. (1987a, 1987b, 1989a, 1989b), and other authors, the flow velocity in the central part of the cavity can be assumed to be parallel in the y-direction. As a result, the flow and temperature fields must be of the following form:

$$u(x, y) = 0; \qquad v(x, y) = v(x) \tag{11}$$

$$T(x, y) = Cy + \theta(x) \tag{12}$$

where C is the unknown but constant temperature gradient in the y-direction.

Eliminating the pressure from Equations 6 and 7 in the usual way and introducing the stream function ψ, it is found that the governing equations become

$$\nabla^2\psi = \mathrm{Da}\,\nabla^4\psi - R\left(\frac{\partial T}{\partial x}\sin\Phi + \frac{\partial T}{\partial y}\cos\Phi\right) \tag{13}$$

$$\nabla^2 T = \frac{\partial\psi}{\partial y}\frac{\partial T}{\partial x} - \frac{\partial\psi}{\partial x}\frac{\partial T}{\partial y} \tag{14}$$

$$u = \frac{\partial\psi}{\partial y}, \quad v = -\frac{\partial\psi}{\partial x} \tag{15}$$

Substituting Equations 11 and 12 into Equations 13 and 14, one obtains, respectively,

$$\frac{d^4v}{dx^4} - \frac{1}{\mathrm{Da}}\frac{d^2v}{dx^2} + \frac{RC}{\mathrm{Da}}v\sin\Phi = 0 \tag{16}$$

and

$$\frac{d^2\theta}{dx^2} = Cv \tag{17}$$

Solutions of Equations 16 and 17 satisfying the boundary conditions given by Equations (9) are

$$v(x) = B(\sinh ax\cos bx - \alpha_0\cosh ax\sin bx) \tag{18}$$

$$T = Cy + B\beta_0(\alpha_0\sinh ax\cos bx + \cosh ax\sin bx) + \frac{v(x)}{2R\sin\Phi} - Cx\cot\Phi \tag{19}$$

where

$$\left.\begin{aligned} &\gamma = \sqrt{4RC\,\mathrm{Da}\sin\Phi}, && a = \sqrt{\frac{\gamma+1}{4\mathrm{Da}}} \\ &\beta = \sqrt{\gamma^2 - 1}, && b = \sqrt{\frac{\gamma-1}{4\mathrm{Da}}} \\ &\beta_0 = \frac{\beta}{2R\sin\Phi}, && B = \frac{\gamma(1 + C\cot\Phi)}{2DC\,\mathrm{Da}} \\ &\alpha_0 = \tanh\frac{a\eta}{2}\cot\frac{b\eta}{2} \\ &D = (a + \alpha_0 b)\cosh\frac{a\eta}{2}\cos\frac{b\eta}{2} + (b - \alpha_0 a)\sinh\frac{a\eta}{2}\sin\frac{b\eta}{2} \\ &E = \alpha_0\sinh\frac{a\eta}{2}\cos\frac{b\eta}{2} + \cosh\frac{a\eta}{2}\sin\frac{b\eta}{2} \\ &Q = B\beta_0 E - \frac{\eta}{2\kappa}(1 + \kappa C\cot\Phi) \end{aligned}\right\} \tag{20}$$

The temperature distribution within the solid boarding wall is obtained by solving the Laplace equation $\nabla^2 T = 0$, with appropriate boundary conditions (Equations 9c and 9d), as

$$T = Cy + \frac{x}{\kappa} + Q \tag{21}$$

The temperature fields, Equations 19 and 21, are only valid in the core region of the cavity and, consequently, are not required to satisfy the thermal boundary conditions at each end of the cavity (Equation 9b). However, these boundary conditions can be indirectly satisfied by matching the core solution with the end regions through the evaluation of the temperature gradient C in the y-direction. Following Bejan (1983), the value of C is obtained by imposing an energy flux condition at the end regions of the enclosure. For the present problem, it may be shown that at any y,

$$C = \frac{1}{\eta + (1 - \eta)\kappa}\int_{-\eta/2}^{\eta/2} v(x)\theta(x)dx \tag{22}$$

Substituting Equations 18 and 19 into Equation 22 and integrating yields

$$\frac{B^2}{8RC\sin\Phi}[(1-\alpha_0^2)F + 2\alpha_0 G + (1+\alpha_0^2)H + 2\eta\alpha_0(\beta-\alpha_0)] + \frac{B\cot\Phi}{a^2+b^2}\left(D\eta - \frac{4ab}{a^2+b^2}E\right) + \kappa(1-\eta) + \eta = 0 \quad (23)$$

where

$$\beta_1 = -\frac{4\,\mathrm{Da}^2}{\gamma}(a^3 - 3ab^2)$$

$$\beta_2 = -\frac{4\,\mathrm{Da}^2}{\gamma}(3a^2b - b^3)$$

$$F = \beta_1 \sinh a\eta \cos b\eta + \beta_2 \cosh a\eta \sin b\eta$$

$$G = \beta_2 \sinh a\eta \cos b\eta - \beta_1 \cosh a\eta \sin b\eta$$

$$H = \eta - \frac{\sinh a\eta}{a} + \frac{\sin b\eta}{b}$$

The temperature gradient C can be obtained for any combination of the controlling parameters R, Da, and Φ by numerically solving the above transcendental equation.

From Equations 10, 19, and 21, the Nusselt number is given by

$$\mathrm{Nu} = \frac{\kappa}{1 + 2\kappa Q} \quad (24)$$

Results and discussion

In this section, we present some representative results to illustrate the effects of the various controlling parameters. First, the case of an inclined single layer of porous medium ($\eta = 1$) will be examined. The importance of the non-Darcian effects on the heat transfer will be discussed. Next, we will consider the case of a porous layer of extension η, boarded by a solid partition thickness $(1 - \eta)$ with finite conductivity.

Case of an inclined single layer of porous medium ($\eta = 1$)

Typical numerical results are presented in Figures 2a–2e for the case of a vertical porous layer ($\Phi = 90°$). Figure 2a, with $R = 10^2$, Fs = 0, and $\mathrm{Da} = 10^{-5}$, represents the streamlines and isotherms of an asymptotic flow regime. At higher Rayleigh numbers the evolution of the flow structure towards the boundary-layer regime can be observed from Figures 2b and 2c, corresponding to $R = 5 \times 10^2$ and 10^3, respectively. The development of the boundary-layer flow regime with an increasing R is clearly illustrated by the increasing steepness of velocity and temperature profiles near the walls, as well as the formation of a plateau in the core region of the two fluid layers. The effects of Darcy number Da can be seen by comparing Figures 2c and 2d, corresponding to $\mathrm{Da} = 10^{-5}$ and 10^{-3}, respectively. It is seen that, as the porosity of the solid matrix (i.e., Da) is increased, the streamlines become relatively more and more sparsely spaced near the solid boundaries. This is due to the fact that the viscous term (Brinkman) becomes gradually more important and slows down the fluid in the neighborhood of the walls. Finally, the effects of the inertia (Fs) are illustrated in Figures 2c and 2e with $R = 10^3$, $\mathrm{Da} = 10^{-5}$, and Fs = 0 and 10^{-1}, respectively. It is observed that the flow regime has reverted from the boundary layer to the asymptotic regime with an increase in Fs.

The Nusselt number for a vertical cavity ($\Phi = 90°$), as predicted by the Darcy–Brinkman model, is plotted in Figure 3 against R for various Da. In the same figure, the analytical solution obtained by Vasseur et al. (1987b), on the basis of Darcy's model, is shown as a dotted line. When $\mathrm{Da} \geq 10^{-4}$, Darcy's law overpredicts the heat transfer across the enclosure due to the neglect of the boundary effects. This is expected since, due to the viscous forces exerted near the solid wall boundaries, Brinkman's model provides a lower flow circulation, which causes less energy to be carried away near the thermally active walls, thus causing a lower Nusselt number. For a given value of Da, the deviation from Darcy's model increases as R becomes larger. The good agreement between the numerical and analytical results of Figure 3 is noted.

Figures 4 and 5 illustrate the combined effects of Brinkman and Forschheimer terms on the Nusselt number through a vertical cavity. Both Darcy and Darcy–Brinkman's solutions are depicted on the graphs for comparison purpose. The results presented in Figure 4 were obtained for $\mathrm{Da} = 10^{-3}$. It is seen that, at a fixed R, the inclusion of the Brinkman–Forschheimer terms in the equation of motion results in lower heat transfer rates than the Darcy solution. As R is increased, the differences between the Darcy and Darcy–Brinkman–Forschheimer solutions become more important. This is expected, since the effects of viscous diffusion and inertia become increasingly important as the flow circulation is enhanced. For a given Rayleigh number $R = 10^3$, Figure 5 illustrates the influence of the Darcy number on the non-Darcian effects. Figure 5 clearly shows that

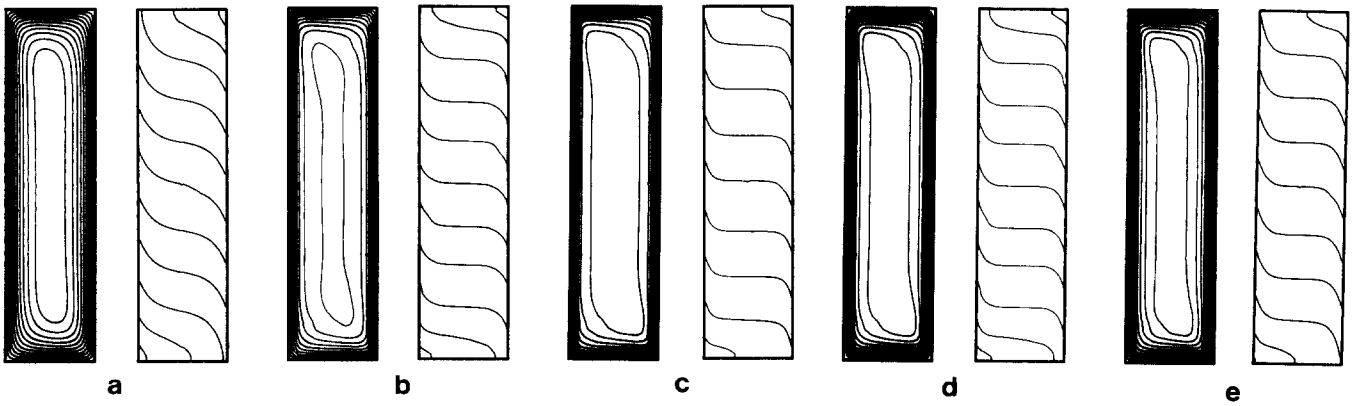

Figure 2 Numerical solutions for the flow and temperature fields, respectively, for a vertical enclosure ($\Phi = 90°$). (a) $R = 10^2$, Fs = 0, $\mathrm{Da} = 10^{-5}$, $\Psi_{max} = 2.350$; (b) $R = 5 \times 10^2$, Fs = 0, $\mathrm{Da} = 10^{-5}$, $\Psi_{max} = 3.586$; (c) $R = 10^3$, Fs = 0, $\mathrm{Da} = 10^{-5}$, $\Psi_{max} = 4.229$; (d) $R = 10^3$, Fs = 0, $\mathrm{Da} = 10^{-3}$, $\Psi_{max} = 4.101$; and (e) $R = 10^3$, $\mathrm{Fs} = 10^{-1}$, $\mathrm{Da} = 10^{-5}$, $\Psi_{max} = 3.506$

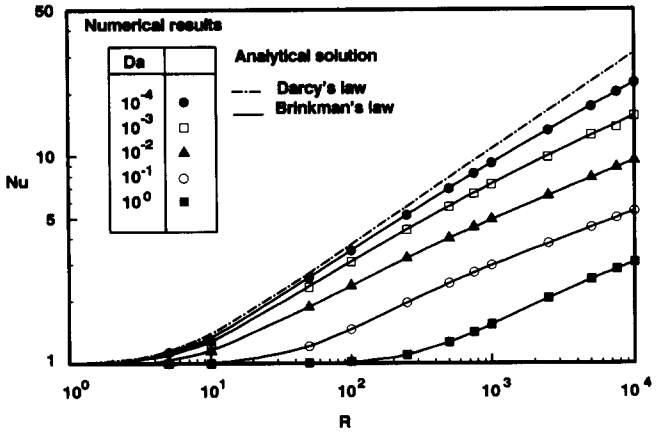

Figure 3 Variation of the Nusselt number versus the Rayleigh number for the Darcy–Brinkman model, $\Phi = 90°$, and $\eta = 1$

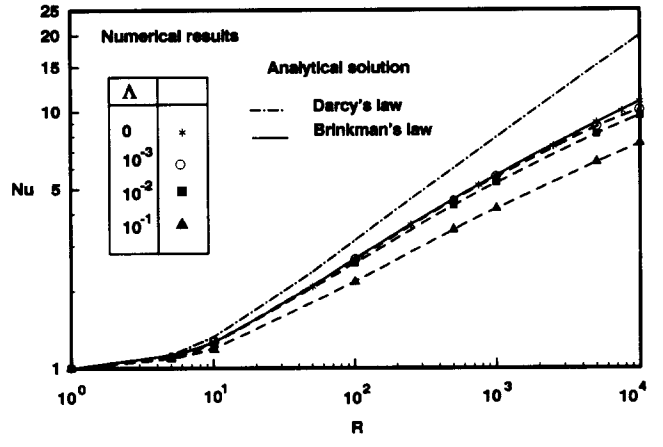

Figure 4 Effect of inertia on the Nusselt number and comparison with Darcy and Darcy–Brinkman solutions, $\Phi = 90°$, $Da = 10^{-3}$, and $\eta = 1$

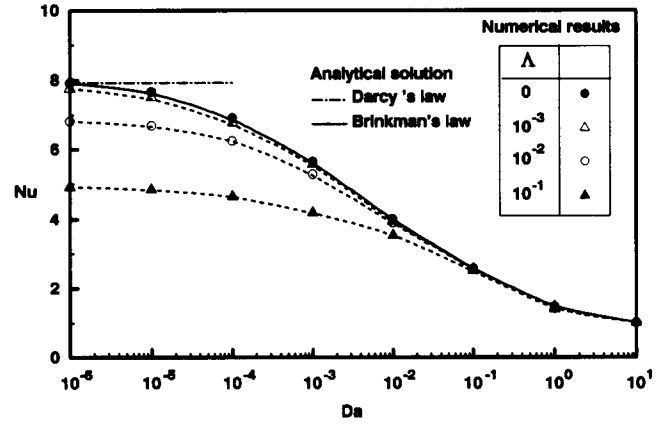

Figure 5 Effect of the Darcy number on the Nusselt number and comparison with Darcy, Darcy–Brinkman and Darcy–Brinkman–Forschheimer solutions, $\Phi = 90°$, $R = 10^3$, and $\eta = 1$

for Darcy numbers less than $Da = 10^{-6}$, there are no variations between the Nusselt number obtained from Darcy's law and the corresponding ones computed by the Brinkman-extended Darcy model. However, for these relatively low values of Da, the inertia effects are important, and utilization of Darcy flow would overpredict the cavity Nusselt number considerably. Thus when $Da = 10^{-6}$, Darcy's solution overpredicts the heat transfer by approximately 14 percent when $\Lambda = 10^{-2}$ and by 38 percent when $\Lambda = 10^{-1}$. As Da is increased, the viscous effects become more important and slow down the buoyancy-induced flow inside the cavity, resulting in a decreasing heat transfer rate. For this situation, the inertial effects are relatively less important, and they become negligible when $Da \geq 10^{-1}$, for which the Darcy–Brinkman–Forschheimer model reduces to the Brinkman-extended Darcy flow model.

Figure 6 presents the results obtained for Nu as a function of the angle of inclination Φ for $R = 10^3$ and $Da = 10^{-3}$. The orientation angle Φ is seen to have a dominant effect on the heat transfer rate. As the angle of inclination Φ approaches 180°, the Nusselt number tends toward unity, since the situation corresponds to the case of a cavity heated from the top, which causes no convection since the density gradient is stable. The Nusselt number increases with decreasing Φ, passes through a peak, and then begins to decrease. The peak in Nusselt number occurs at about 60° for Darcy's law, but at about 50° for the Brinkman-extended Darcy model. With the Darcy–Brinkman–Forschheimer model, the peak in Nu shifts from about 40° to 60° as the parameter Λ is increased from 10^{-3} to 10^{-1}. As expected, the non-Darcian effects are found to be more important when the flow circulation within the cavity is strong, i.e., for $30° \leq \Phi \leq 90°$.

Case of a porous layer boarded by a solid wall

We consider now the case of a vertical ($\Phi = 90°$) porous layer extension η, boarded by a solid wall of thickness $(1 - \eta)$. Figure 7 shows the streamline and isotherm contour plots at

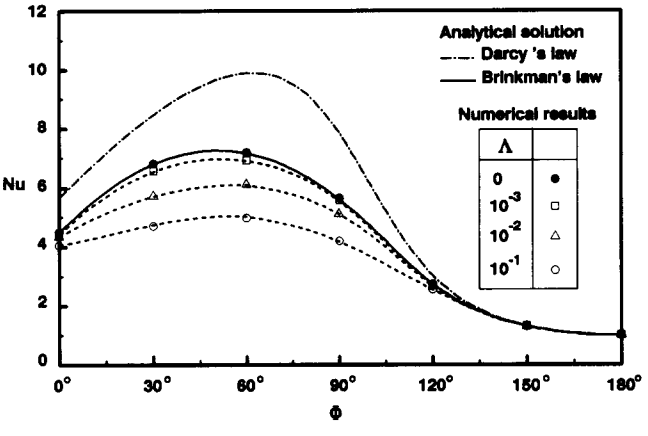

Figure 6 Effect of inclination angle on the Nusselt number and comparison with Darcy, Darcy–Brinkman, and Darcy–Brinkman–Forschheimer solutions, $R = 10^3$, $Da = 10^{-3}$, and $\eta = 1$

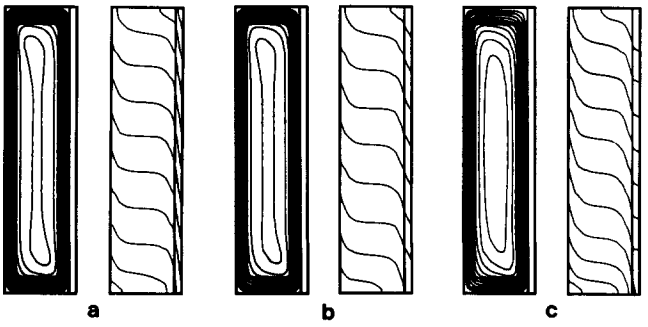

Figure 7 Numerical solution for the flow and temperature fields, respectively, for a vertical enclosure ($\Phi = 90°$) with $R = 5 \times 10^2$, $\eta = 0.9$, $Da = 10^{-3}$, $\Lambda = 0$, and (a) $\kappa = 0.5$, $\Psi_{max} = 3.379$; (b) $\kappa = 2.0$, $\Psi_{max} = 3.579$; and (c) $\kappa = 10.0$, $\Psi_{max} = 4.620$

$R = 5 \times 10^2$ for a vertical porous layer ($Da = 10^{-3}$, $\Lambda = 0$) of extension $\eta = 0.9$ boarded by a solid slab for $\kappa = 0.5$, 2.0, and 10.0. The corresponding maximum stream function values are 3.379 for $\kappa = 0.5$, 3.579 for $\kappa = 2.0$, and 4.620 for $\kappa = 10.0$. Thus the strength of circulation is increased with increasing κ. The resulting heat transfer through the system, as predicted by Equations 23 and 24, is presented in Figure 8 as a function of R and κ. Verification of the results of analysis by numerical computation is also indicated on the graph. Figure 8 shows that, for a given value of R, the Nusselt number is enhanced as κ is made larger. This is expected, since for $\kappa \ll 1$ the solid slab behaves as an insulating plate such that $Nu \to 1$. As κ (i.e., the relative conductivity of the solid wall) increases, the convection and the resulting heat transfer within the porous layer are both enhanced. It must be mentioned that the limit κ very large corresponds to the case of a porous layer boarded by an isothermal wall of finite thickness. The thermal boundary conditions applied on the porous layer are thus a constant heat flux on one side and an isothermal wall on the other side. For this situation the present theory is inapplicable, since there is no reason to expect that the resulting flow field, within the porous layer, should be parallel. For this reason, the limit κ very large is not discussed in this paper.

The effects of inertia ($\Lambda > 0$) on the present system are illustrated in Figures 9 and 10. Figure 9 presents the heat transfer as a function of η for $R = 10^4$, $Da = 10^{-3}$, and $\kappa = 1$. The limit $\eta \to 0$ corresponds to a solid slab, for which $Nu = 1$, while $\eta \to 1$ corresponds to a single layer of porous medium.

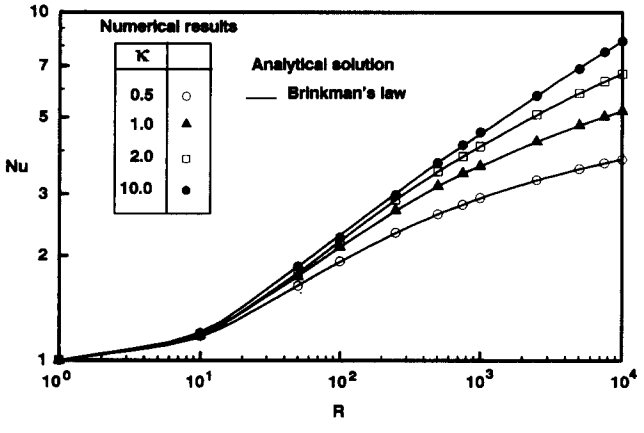

Figure 8 Heat transfer through a vertical porous layer bordered by a solid wall: effect of conductivity ratio κ, $\Lambda = 0$, $\eta = 0.9$, and $Da = 10^{-3}$

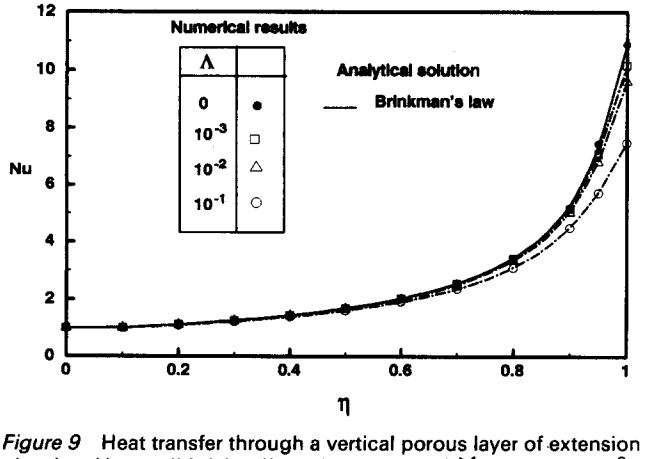

Figure 9 Heat transfer through a vertical porous layer of extension η bordered by a solid slab: effect of inertia, $R = 10^4$ and $Da = 10^{-3}$

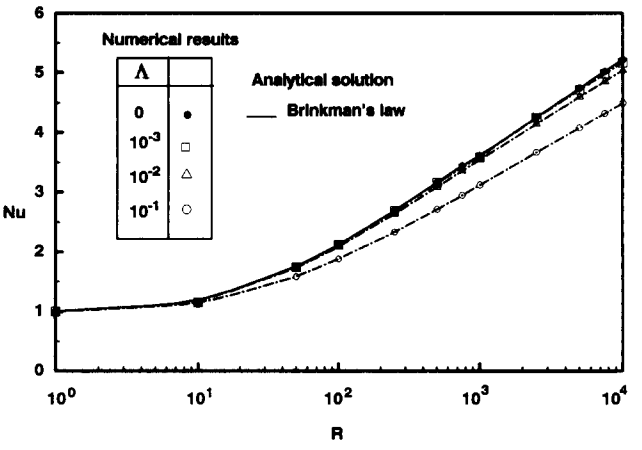

Figure 10 Heat transfer through a vertical porous layer bordered by a solid wall: effect of inertia, $\eta = 0.9$, $Da = 10^{-3}$, and $\kappa = 1$

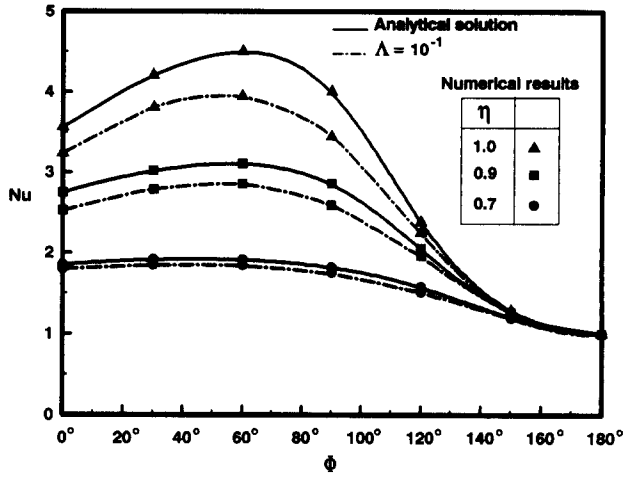

Figure 11 Effect of inclination angle and inertia on the Nusselt number for various η, $R = 10^3$, $Da = 10^{-2}$

In general, Nu increases monotonically with η, since the natural-convection heat transfer is enhanced as the thickness of the porous layer is made larger. The heat transfer as a function of R is illustrated in Figure 10 for $\eta = 0.9$, $Da = 10^{-3}$, and $\kappa = 1$. In the absence of inertia forces ($\Lambda = 0$), both Figures 9 and 10 indicate that the Brinkman's law predicted by the present analytical solution is in good agreement with the numerical results. In fact, apart from the case with $\Lambda = 10^{-1}$, the inertia effects are seen to be almost negligible for the composite system considered here.

Figure 11 illustrates the effect of the inclination Φ on Nusselt number for $R = 10^3$, $Da = 10^{-2}$, and various values of the porous-layer thickness η. The solid lines represent the analytical solution predicted on the basis of the Brinkman-extended Darcy's law, i.e., in the absence of inertial effects ($\Lambda = 0$). The numerical results, obtained when $\Lambda = 10^{-1}$ (i.e., when the inertial effects are relatively important), are presented in Figure 11 as dashed lines. As expected, for a given orientation Φ, the inertial effects are maximum when $\eta = 1.0$, i.e., when the thickness of the porous layer is maximum. As the value of η is decreased the convective motion within the system is progressively inhibited and the inertial effects become relatively less important. Thus, Figure 11 indicates that inertia becomes almost negligible when $\eta \leq 0.7$, and consequently the present analytical solution, based on the Brinkman-extended Darcy's law, predicts correctly the heat transfer.

Conclusions

The solution of the natural-convection heat transfer in an inclined porous layer boarded by a wall of finite thickness is derived. In a parametric study, the dependence of the Nusselt number on the governing parameters R, Da, Φ, Λ, η, and κ is investigated. The following conclusions can be made.

Single layer of porous medium ($\eta = 1$)

(1) The effects of the no-slip boundary condition have been studied both theoretically and numerically using the Brinkman-extended Darcy model. The boundary effects are found to slow down the buoyancy-induced flow with a resulting decrease in heat transfer. This trend is made larger as the permeability of the porous medium is enhanced. The present analytical solution reduces to the regular Darcy's law in the limit of low porosity. A good agreement is found between the analytical predictions and a numerical simulation of the same phenomenon conducted for a wide range of the governing parameters.

(2) The effects of the inertia have been studied numerically using the Brinkman–Forschheimer–extended Darcy model. In general, the inclusion of the Forschheimer term (Λ) in the momentum equation leads to a reduction of the heat transfer rate. However, the boundary effects (Da) are, in general, the most significant.

(3) The orientation angle Φ is found to have a dominant effect on the heat transfer rate. The peak in Nu occurs at about 60° for Darcy's law, but it is at about 50° for the Brinkman-extended Darcy's model. With the Darcy–Brinkman–Forschheimer model, the peak in Nu shifts from about 40° to 60° as Λ is increased from 10^{-3} to 10^{-1}.

Porous layer boarded by a solid slab

The heat transfer through a porous layer of extension η, boarded by a solid wall of thickness $(1 - \eta)$, has been also considered. In the absence of inertia effects (Λ), the analytical solution was found to be in good agreement with the numerical results. It was found that the heat transfer increases considerably with an increase of the conductivity ratio κ. The inertia effects in such a system were found to be relatively weak, especially when $\eta \leq 0.8$. For a given orientation Φ, the inertial effects become progressively negligible as the relative thickness η of the porous layer is made smaller than approximately 0.7.

Acknowledgments

This work was supported in part by the Natural Sciences and Engineering Research Council of Canada and jointly by the FCAR Government of Quebec.

References

Bejan, A. 1983. The boundary layer regime in a porous layer with uniform heat flux from the side. *Int. J. Heat Mass Transfer*, **26**, 1339–1346

Beckerman, C., Viskanta, R., and Ramadhyani, A. 1986. Numerical study of non-Darcian natural convection in a vertical enclosure filled with a porous medium. *Numer. Heat Transfer*, **10**, 557–570

Bories, S. A. and Combarnous, M. A. 1973. Natural convection in a sloping porous layer. *J. Fluid Mech.*, **57**, 63–79

Chan, B. K. C., Ivey, C. M., and Barry, J. M. 1970. Natural convection in enclosed porous media with rectangular boundaries. *J. Heat Transfer*, **2**, 21–27

Cheng, P. 1978. Heat transfer in geothermal systems. *Adv. Heat Transfer*, **14**, 1–105

Combarnous, M. and Bories, S. 1975. Hydrothermal convection in saturated porous media. *Adv. Hydrosci.*, **10**, 231–307

Cormack, D. E., Leal, L. G., and Inberger, J. 1974. Natural convection in a shallow cavity with differentially heated end walls. Part 1, Asymptotic theory. *J. Fluid Mech.*, **65**, 209–230

Forschheimer, P. 1901. Wasserbewegung durch Boden. *ForschHft. Ver Dt. Ing.*, **45**, 1782–1788

Klarsfeld, S. 1970. Champs de température associés aux mouvements de convection naturelle dans un milieu poreux limité. *Rev. Gén. Therm.*, **9**, 1403–1423

Lauriat, G. and Prasad, V. 1987. Natural convection in a vertical porous cavity—A numerical study for Brinkman-extended Darcy formulation. *J. Heat Transfer*, **109**, 681–696

Lauriat, G. and Prasad, V. 1989. Non-Darcian effects on natural convection in a vertical porous enclosure. *Int. J. Heat Mass Transfer*, **32**, 2135–2148

Patankar, S. V. 1980. *Numerical Heat Transfer and Fluid Flow*. Hemisphere/McGraw-Hill, Washington, DC

Poulikakos, D. 1985. A departure from the Darcy model in boundary layer natural convection in vertical porous layer with uniform heat flux from the side. *J. Heat Transfer*, **107**, 716–720

Poulikakos, D. and Bejan, A. 1985. The departure from Darcy flow in natural convection in a vertical porous layer. *Phys. Fluids*, **28**, 3477–3484

Seki, N., Fukusako, S., and Inaba, H. 1978. Heat transfer in a confined rectangular cavity packed with porous media. *Int. J. Heat Mass Transfer*, **21**, 985–989

Sen, A. K. 1987. Natural convection in a shallow porous cavity—The Brinkman model. *Int. J. Heat Mass Transfer*, **30**, 855–868

Tong, T. W. and Subramanian, E. 1985. A boundary layer analysis for natural convection in vertical porous enclosure—Use of the Brinkman-extended Darcy model. *Int. J. Heat Mass Transfer*, **28**, 563–571

Vasseur, P. and Robillard, L. 1987a. The Brinkman model for boundary layer regime in a rectangular cavity with uniform heat flux from the side. *Int. J. Heat Mass Transfer*, **30**, 717–727

Vasseur, P., Satish, M. G., and Robillard, L. 1987b. Natural convection in a thin, inclined porous layer exposed to a constant heat flux. *Int. J. Heat Mass Transfer*, **30**, 537–549

Vasseur, P., Wang, C. H., and Sen, M. 1989a. The Brinkman model for convection in a shallow porous cavity with uniform heat flux. *Numer. Heat Transfer*, **15**, 221–242

Vasseur, P., Wang, C. H., and Sen, M. 1989b. Thermal instability and natural convection in a fluid layer over a porous substrate. *Wärme- und-Stoff übertragrung*, **24**, 337–347

Walker, K. L. and Homsy, M. G. 1978. Convection in a porous cavity. *J. Fluid Mech.*, **87**, 449–474

Weber, J. E. 1975. The boundary layer regime for convection in a vertical porous layer. *Int. J. Heat Mass Transfer*, **18**, 569–573